Determining the Timing and Rate of Laurentide Ice Sheet Thinning During the Last Deglaciation in New England with ^{10}Be Dipsticks

A thesis proposal prepared by

Christopher Halsted

In partial fulfillment of the requirements for a
Masters of Science in Geology
in the Department of Earth and Environmental Sciences
at Boston College

Thesis Advisor: Dr. Jeremy Shakun

Committee Member: Dr. Noah Snyder

Committee Member: Dr. Ethan Baxter

1. Introduction

Depicting the mechanistic relationships between surface air temperatures, ice sheet ablation rates, and ocean circulation is one of the primary challenges facing ice sheet and climate modelers (Stokes et al., 2015). Paleo-ice sheet reconstructions are one of the best ways to understand these relationships, as they allow model simulations to be validated by reconciling against direct measurements or proxy records. As the largest ice sheet during the last glacial maximum, the Laurentide ice sheet (LIS) is of particular interest to ice sheet modelers, as its complete retreat contributed 60-90 m of sea level rise (Clark and Mix, 2002) and likely influenced global climate by disrupting the Atlantic meridional overturning circulation (AMOC; Clark et al., 2001; Liu et al., 2009; Shakun et al., 2012). However, while LIS extent histories are precise and numerous (e.g. Balco et al., 2002; Dyke, 2004; Carlson et al., 2007; Ridge et al., 2012), LIS thickness histories are sparse and full of uncertainty (e.g. Spear et al., 1994; Rogers, 2003; Davis et al., 2015; Koester et al., 2017a). Without a robust thinning history, the mechanistic relationships between LIS mass loss, sea level rise, AMOC variations, and abrupt climate shifts will remain poorly understood.

The predominantly flat terrain which the LIS overrode prevents such a history from being created in most regions, but the mountains of New England are ideally situated to capture the thinning history of the southeastern LIS. In this project I will calculate cosmogenic exposure ages at various elevations on mountains throughout New England, creating a series of chronometric exposure dipsticks to track the lowering surface of the southeastern LIS. There are currently only three published LIS dipsticks (Davis et al., 2015; Koester et al., 2017a; Koester et al., 2017b), but this project aims to construct 8 more dipsticks and refine the southeastern LIS thinning history.

2. Background

2.1. Deglacial Paleoclimate and Sea Level

The last deglacial period featured complex shifts in surface temperatures, atmospheric CO_2 concentration, and sea level rise rates. In order to understand the implications and context of a southeastern LIS thinning history, it is essential to understand the evolution of the deglacial paleoclimate, AMOC strength, and sea level.

2.1.1. Last Glacial Maximum to Heinrich Stadial I (23 – 19 ka)

Most Northern Hemisphere (NH) ice sheets reached their full extents between 26.5 – 23 ka (Balco et al., 2002; Clark et al., 2009), a period which overlaps the last boreal summer insolation (BSI) minimum (~24 ka; Abe-Ouchi et al., 2013). A subsequent BSI rise forced a gradual NH temperature increase starting around 21.5 ka (Liu et al., 2009), initiating retreat of southern ice margins (Carlson and Winsor, 2012). LIS meltwater funneled into the North Atlantic suppressed thermohaline circulation, reducing AMOC strength (Fig. 1) and northward heat transport (Clark et al., 2001; Liu et al., 2009; Clark et al., 2012). This created a bipolar see-saw effect where NH temperatures dropped while Southern Hemisphere (SH) temperatures rose (Carlson and Clark, 2012; Shakun et al., 2012), initiating Heinrich Stadial I (HS1, also known as the Oldest Dryas).

2.1.2. Heinrich Stadial 1 (19-14.6 ka)

Rising SH temperatures during HS1 resulted in the removal of sea ice from the mid southern latitudes and a release of CO_2 due to wind-driven upwelling of the now-exposed Southern Ocean (Denton et al., 2010; Shakun et al., 2012). In the NH, reduced northward heat transport to the North Atlantic caused an expansion of winter sea-ice, resulting in extremely low winter surface air temperatures and a highly seasonal climate (Broecker, 2006; Denton et al., 2010; Buizert et al., 2014).

Sea level rose slowly during the first part of HS1 (2-4.5 mm yr^{-1}), but accelerated dramatically to ~12 mm yr^{-1} from 16.5 – 15 ka (Fig. 1; Lambeck et al., 2014). As the LIS and other NH ice sheets were exhibiting trends of decreasing meltwater flux during this period (Liu et al., 2009), this acceleration is believed to have been sourced primarily from the SH, where interstadial conditions had initiated substantial melting on Antarctica (Denton et al., 2010).

2.1.3. Bølling-Allerød Warm Period (14.6 – 12.9 ka)

HS1 ended abruptly around 14.6 ka as an unprecedented sea level rise event dramatically altered oceanic conditions. Meltwater Pulse 1a (MWP-1A, 14.6 – 14.3 ka) featured the fastest sea level rise of the deglacial period, with 8-15 m gained over a ~300 year period (Fig. 1; Lambeck et al., 2014; Liu et al., 2016). The contribution from individual ice sheets to MWP-1A is debated, with some models indicating that it was sourced primarily from the LIS (Peltier, 2005) and others attributing only 50% of the sea level rise to NH ice sheets with the remainder coming from Antarctica (Deschamps et al., 2012). MWP-1A was synchronous with a rapid strengthening of the AMOC (Fig. 1) raising temperatures in the North Atlantic and initiating the Bølling-Allerød warm period (B-A; Liu et al., 2009). The rest of this period was characterized by a reversal of the bi-polar see-saw, accelerated LIS retreat, and rapid sea level rise (Fig. 1 & 2; Ridge et al., 2012; Carlson and Clark, 2012; Lambeck et al., 2014).

2.1.4. Younger Dryas (12-9-11.7 ka)

The B-A ended abruptly around 12.9 ka, when a sudden AMOC reduction similar to that which preceded HS1 stifled northward oceanic heat transport and led to a drop in NH temperatures (Fig. 1; Broecker, 2006; Clark et al., 2012; Buizert et al., 2014). The following stadial period is known as the Younger Dryas (YD), and in the NH is associated with expansive

sea-ice, extremely cold winters, and a slowing of ice retreat (Dyke, 2004; Broecker, 2006; Ridge et al., 2012; Buizert et al., 2014).

2.2. Southeastern Laurentide Ice Sheet Retreat History

LIS extent histories have so far employed radiocarbon dating (e.g. Dyke, 2004), periglacial lake varve records (e.g. Ridge et al., 2012), and *in-situ* cosmogenic nuclide exposure dates (e.g. Balco et al., 2002; Carlson et al., 2007), with thousands of data points. LIS thickness histories, on the other hand, are based on only a handful of data points, isostatic-inversion geophysical models (Clark and Tarasov, 2014; Peltier et al., 2015), and numerical ice sheet models (Gregoire et al., 2012; Abe-Ouchi et al., 2013).

2.2.1. Ice Extent

The southeastern LIS margin reached its maximum extent around 23.3 ± 0.5 ka, and began retreating at 21.1 ± 0.4 ka in response to increasing BSI (Balco et al., 2002; Liu et al., 2009; Carlson and Winsor, 2012). LIS retreat slowed during HS1 (50-100 m yr^{-1}), briefly stalling and readvancing around 17.2 ka. Following MWP-1A, retreat accelerated dramatically and assumed an average pace of 300 m yr^{-1} until the YD, with the only interruption being a minor readvance around 14 ka (Fig. 2). Ice retreat slowed following the onset of the YD, but the ice margin had by this time retreated entirely out of New England (Dyke, 2004; Ridge et al., 2012).

2.2.2. Ice Thickness

Initial attempts to record a southeastern LIS thinning history produced six ^{14}C ages from lake and bog basal sediments in the White Mountains, NH meant to determine minimum-limiting ages for the lowering of the ice surface in the region. However, the results contained so much scatter and uncertainty that it is impossible to tell the timing and rate of ice thinning (Table 1; Davis and Davis, 1980; Spear, 1989; Spear et al., 1994; Rogers, 2003).

Preliminary cosmogenic exposure ages have yielded more conclusive results, with dipsticks providing evidence of rapid ice thinning and retreat in central Maine (~16-15 ka; Davis et al., 2015), the White Mountains (starting ~17 ka; Koester et al., 2017a), and on the Maine coast (15.2 ± 0.7 ka; Koester et al., 2017b). It should be noted that the dipsticks from central and coastal Maine feature broad 90% confidence intervals, preventing the exclusion of more complex thinning histories with varying thinning rates. Furthermore, cosmogenic exposure ages from the highest summits in this region are erroneously old, likely due to the incomplete removal of cosmogenic nuclides from prior episodes of exposure by non-erosive, cold-based ice (Bierman et al., 2015; Koester et al., 2017a); they therefore cannot be meaningfully interpreted.

Terrestrial Cosmogenic Nuclide Systematics

Cosmogenic nuclides will be used in this project to measure ice thinning, so this section will provide an overview of cosmogenic exposure dating systematics and its use in glacial chronologies.

2.2.3. Terrestrial Cosmogenic Nuclides and Glacial Chronologies

Terrestrial *in-situ* cosmogenic nuclides (TCNs) are rare isotopes created during nuclear reactions between terrestrial atoms in surface minerals and high-energy cosmic rays or secondary cosmic particles (i.e. neutrons and protons cast off by cosmogenic reactions in the atmosphere). TCNs accumulate predictably in minerals at or near the Earth's surface, allowing surface exposure ages to be calculated by measuring their present concentration and dividing by their production rate since their initial accumulation. One of the most useful properties of TCNs is the exponential drop in production with depth in any material; below 2 m of bedrock, there is virtually no TCN production (Phillips et al., 1986; Lal, 1991; Gosse and Phillips, 2001). This makes TCN exposure dating particularly appealing for glacial chronologies due to the abundance

of glacially-eroded bedrock and boulders left in the wake of retreating ice margins. Minerals on these glacially-scoured surfaces likely had negligible nuclide concentrations at the onset of deglaciation, so their concentration of TCNs can be used to infer the timing of ice retreat (Fig. 3; Nishiizumi et al., 1991; Balco, 2011).

2.2.4. Limitations and Pitfalls

Unfortunately, a potential pitfall in using TCN exposure ages for glacial chronologies is this assumption that a glacially-scoured surface was not exposed to cosmic rays prior to ice retreat. In regions dominated by a 'warm' basal regime, where the basal temperature is above freezing and a lubricating layer of meltwater forms, this is generally a safe assumption. Warm-based ice sheets are powerful agents of erosion, easily capable of removing the top 2 m of TCN-rich surface bedrock when advancing, bringing previously unexposed minerals to the surface (Fig. 3; Balco, 2011). However, in regions dominated by 'cold-based' ice, where the basal temperature is below freezing and the base of the ice sheet is frozen to the underlying bed, far less glacial erosion occurs (Paterson, 1994; Payne, 1995) and there is a greater chance that sampled material will contain TCNs from previous exposures, leading to falsely old exposure ages (Fig. 3; Balco, 2011).

2.2.5. Special Considerations for New England

The largest source of uncertainty in TCN exposure age calculations comes from estimating TCN production rates, which vary with elevation and latitude (Lal, 1991; Gosse and Phillips, 2001; Balco, 2011). However, a regional ^{10}Be calibration data set has been constructed for the northeastern US by reconciling ^{10}Be exposure ages with published radiocarbon dates, substantially increasing precision and accuracy in exposure ages for the region (Balco et al., 2009). For this reason, ^{10}Be will be used to construct the dipsticks in this project.

3. Research Approach

^{10}Be is primarily used in glacial chronologies to date glacially-transported boulders located on moraines and track the horizontal movements of ice margins (e.g. Balco et al., 2002), but it can also be used to date boulders and scoured bedrock at various elevations on a mountain, turning the mountain into a chronometric "dipstick" that tracks a lowering ice surface (e.g. Koester et al., 2017b). This method relies on two assumptions: (1) Glacial erosion left the boulders and bedrock with surfaces devoid of ^{10}Be from previous exposures and (2) the overlying ice sheet shielded the surfaces from cosmic rays until thinning caused the ice surface to lower below their elevations. If these assumptions are valid, then the date of exposure calculated for each boulder or bedrock surface will indicate the time at which the ice surface was at that elevation. By calculating the date of exposure for samples at various elevations in a vertical transect, a dipstick depicting the timing and rate of ice thinning can be constructed (Fig. 4 & 5). Where topography allows, this is currently the most precise and applicable method for generating a measurement-based ice thinning history (Bierman, 2007).

While the LIS predominantly overrode flat terrain, the mountains of New England, southern Quebec, and the eastern Canadian Arctic provide sufficient topographic relief for dipstick construction. However, the polar climate of the eastern Canadian Arctic may have been conducive to cold-based ice during the last glaciation (Sugden, 1978; Briner et al., 2003), posing an inheritance risk for ^{10}Be exposure ages. Therefore, New England and southern Quebec represent the only regions with the necessary topography and climate for successful LIS dipstick construction. In this project, I will construct dipsticks using nine mountains around New England (Fig. 6) to constrain the LIS thinning history of the region.

The specific mountains chosen for dipstick construction generally have the largest prominence in their respective ranges to capture the largest possible ice thinning history. Because dipsticks have already been constructed for Mt. Washington, Mt. Katahdin, and Cadillac Mountain, I targeted several other significant peaks in New England (Fig. 6) for maximum spatial coverage of the region. These peaks are (elevations in meters in parentheses): Wachusett Mountain, MA (611), Mt. Greylock, MA (1,064), the Catskill Mountains, NY (1,270), Mt. Monadnock, NH (965), Killington Mountain, VT (1,291), Mt. Mansfield, VT (1,339), Jay Peak, VT (1,177), Mt. Lafayette, NH (1,600), and West Bigelow Mountain, ME (1,263).

4. Objectives

By generating a more precise and accurate thinning history for the southeastern LIS during the last deglaciation, I hope to answer several lingering questions:

(1) When did ice thinning occur at various latitudes throughout New England? As demonstrated by the lack of ice thickness measurements, there is a substantial amount of uncertainty in the timing of ice thinning in this region, which would have had significant effects on meltwater flux, ocean circulation, and downstream effects on climate.

(2) Did the southeastern LIS thinning rate vary during its deglaciation? The last deglacial period encompassed several warm and cold periods, but current thinning histories are not sufficiently precise to determine if the southeastern LIS thinning rate varied during these periods. Of particular interest is the behavior of the LIS during MWP-1A, the source of which is still debated (Peltier, 2005; Deschamps et al., 2012).

(3) What exactly is the relationship between southeastern LIS ablation rates and the AMOC? While AMOC strength appears to have responded to changes in the magnitude and direction of the LIS meltwater flux (Clark et al., 2001; Liu et al., 2009), a causal relationship

between the two variables has not been established. New England varve records suggest a direct, positive correlation between LIS meltwater flux and AMOC strength (Ridge et al., 2012), while a seawater $\delta^{18}O$ record from the North Atlantic suggests the opposite relationship, with increased southeastern LIS meltwater flux leading to a reduced AMOC and colder North Atlantic temperatures (Obbink et al., 2010). By refining the southeastern LIS thinning history, this relationship may become clearer.

(4) How well do ice sheet models depict the southeastern LIS deglaciation? The lack of robust ice-thickness histories has forced LIS reconstructions to rely on glaciological modeling to simulate the three-dimensional retreat of the southeastern LIS (Lambeck et al., 2002; Peltier, 2004; Gregoire et al., 2012). By ground-truthing the thinning history of the southeastern LIS, my data could be used to test the validity of such models.

5. Methods

This project will consist of five distinct stages: sample collection, mineral separation, chemical processing, isotopic measurement, and statistical analysis. ^{10}Be forms primarily in quartz (Gosse and Phillips, 2001), so samples consist of glacially-transported boulders or polished bedrock surfaces with an observable quartz component. Samples are pulverized and sieved to obtain 250-850 μm fragments, and then a combination of physical and chemical separation methods are used to isolate quartz from all other mineral phases (see Corbett et al., 2016). The purified quartz will then be taken to the University of Vermont Cosmogenic Nuclide Lab for chemical processing. This involves digestion of the quartz in HF and the addition of a ^{9}Be carrier, after which anions and cations are separated via column chromatography. The now-isolated Be component of the sample is converted to a solid, BeO form for isotopic analysis on an accelerated mass spectrometer (AMS; Corbett et al., 2016).

The samples for this thesis will be sent to the Purdue Rare Isotopes Measurement Lab (PRIME) for isotopic measurement. The AMS at PRIME measures the ratio between the cosmogenic nuclide of interest (^{10}Be) and a stable isotope added as a carrier during chemical processing (^{9}Be). Because the carrier mass is known for each sample, the ^{10}Be concentration can be calculated for each sample given an isotopic ratio. ^{10}Be concentrations and sample site parameters (GPS coordinates, elevation, topographic shielding factor) are then entered into a free, online exposure age calculator (CRONUS-Earth; Balco et al., 2008) to complete the exposure age calculation. Once all exposure ages for a given mountain are calculated, Monte Carlo simulations will be performed to place probabilistic estimates on the timing and rate of ice thinning in that location.

6. Timeline

Stage	Start Date	End Date	Complete?
Sample Collection	Aug., 2016	Aug., 2017	Yes
Mineral Separation	June, 2017	Oct., 2017	Yes
Chemical Processing	Sept., 2017	Nov., 2017	No
Isotopic Analysis	Dec., 2017	Dec., 2017	No
Statistical Analysis	Jan., 2018	Spring, 2018	No

7. Figures

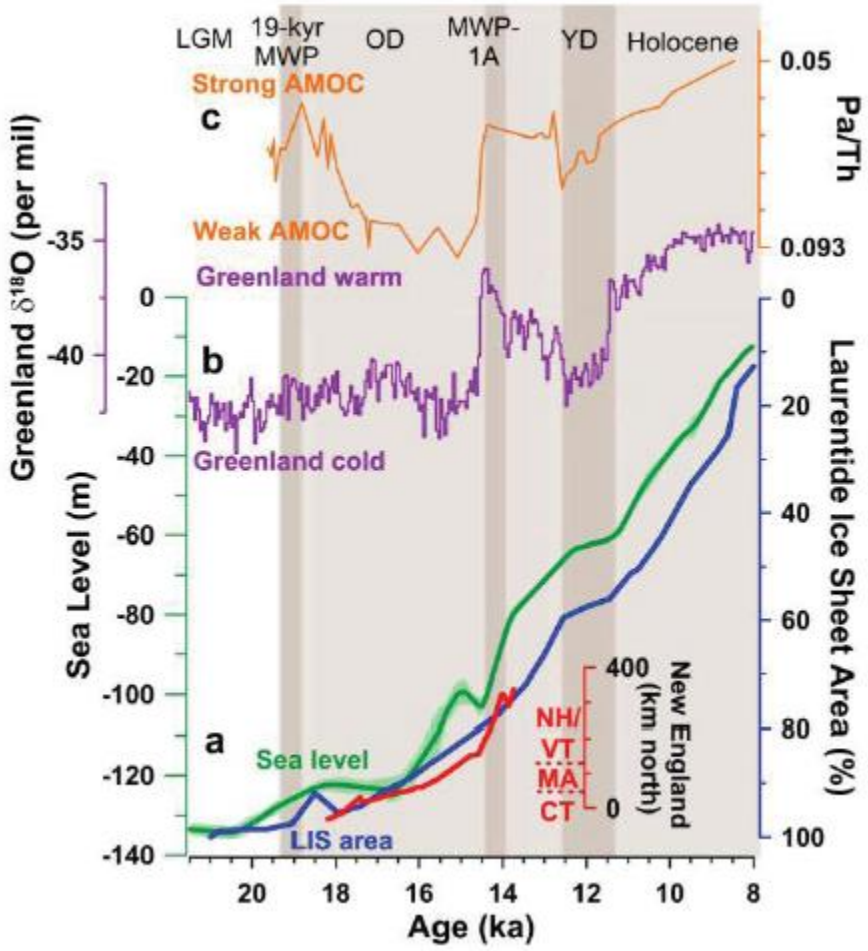

Figure 1: **Proxy reconstructions depicting ice melt, climate, and ocean circulation during the last deglacial period (courtesy of Dr. Jeremy Shakun).** (a) Global sea level (green, from Lambeck et al., 2014). LIS areal retreat (blue, from Dyke, 2004), and retreat of the southeastern LIS margin (red, based on the New England Varve Chronology, Ridge et al., 2012). (b) Greenland $\delta^{18}O$, a proxy for temperature (NGRIP members, 2004). (c) AMOC strength based on protactinium/thorium ratios in a sediment core from the North Atlantic (McManus et al., 2004). Note: In this figure Heinrich Stadial I is referred to as the Oldest Dryas (OD), the two titles are interchangeable and refer to the same period.

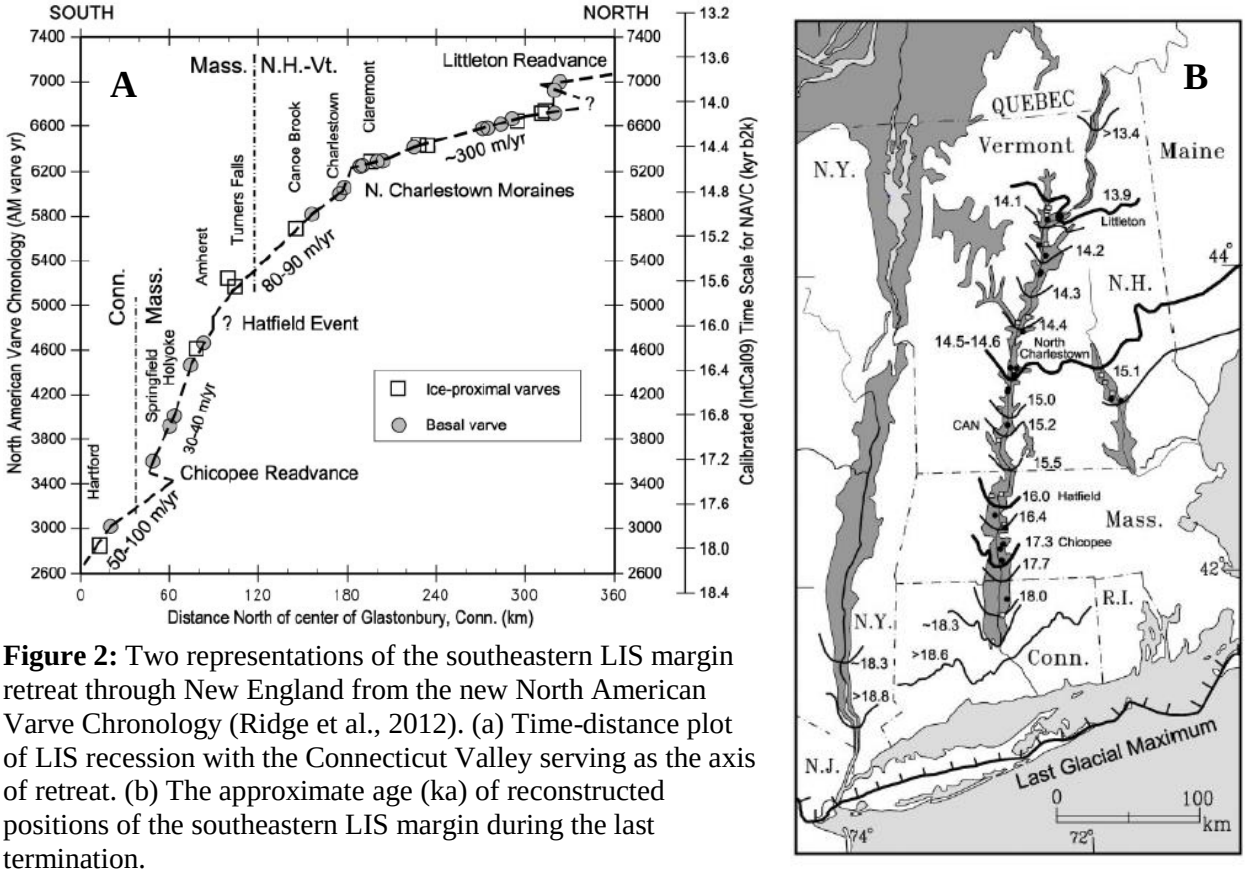

Figure 2: Two representations of the southeastern LIS margin retreat through New England from the new North American Varve Chronology (Ridge et al., 2012). (a) Time-distance plot of LIS recession with the Connecticut Valley serving as the axis of retreat. (b) The approximate age (ka) of reconstructed positions of the southeastern LIS margin during the last termination.

Site	Elev (m)	^{14}C Age	cal yr BP	Source
Moosilauke				
Deer Lake bog	1325	13,000 ± 400	14,195-16,820	Spear (1989)
Mirror Lake	213	13,800 ± 560	15,720-17,415	Davis and Davis (1980)
Franconia Notch				
Lonesome Lake	831	10,535 ± 495	11,065-13,355	Spear et al. (1994)
Profile Lake	593	10,660 ± 40	12,772-12,885	Rogers (2003)
Mt. Washington				
Lakes of Clouds	1538	11,530 ± 165	10,790-13,355	Spear (1989)
Lost Pond	625	12,870 ± 370	14,580-15,760	Spear et al. (1994)

Table 1: Organic ^{14}C age elevational pairs from the White Mountains, NH. These ^{14}C ages were collected in an attempt to constrain the ice thinning history in the region. Each age records the timing of revegetation in the sample location, and thus represents a minimum-limiting date for the ice surface vacating that location.

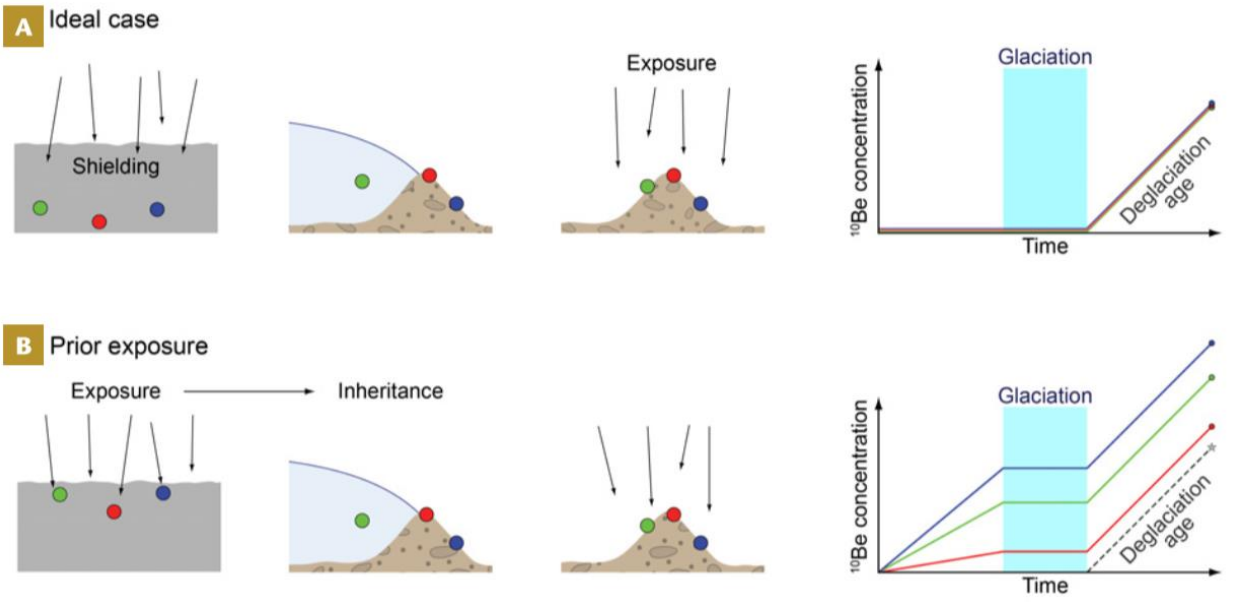

Figure 3: Terrestrial *in-situ* cosmogenic nuclide schematics applied to glacial chronologies. (a) In an ideal case, mineral grains (green, red, and blue dots) are buried below the attenuation depth of cosmogenic reactions prior to glaciation and do not accumulate any cosmogenic nuclides (note ^{10}Be concentration in righthand plot). Glacial erosion removes overlying material, exposing these mineral grains at the surface following ice retreat. ^{10}Be begins to accumulate when ice retreats, recording the age of deglaciation. (b) If cold-based ice overrode the material during glaciation, only a limited amount of erosion would have occurred. This means that mineral grains currently exposed at the surface were located near the surface to begin with (see locations in lefthand picture), meaning that they were exposed to cosmic rays to some extent prior to glaciation and accumulated cosmogenic nuclides during this time. Because of this, they will have a higher ^{10}Be concentration than samples that had never been exposed prior to deglaciation, and give falsely old ages (see righthand plot).

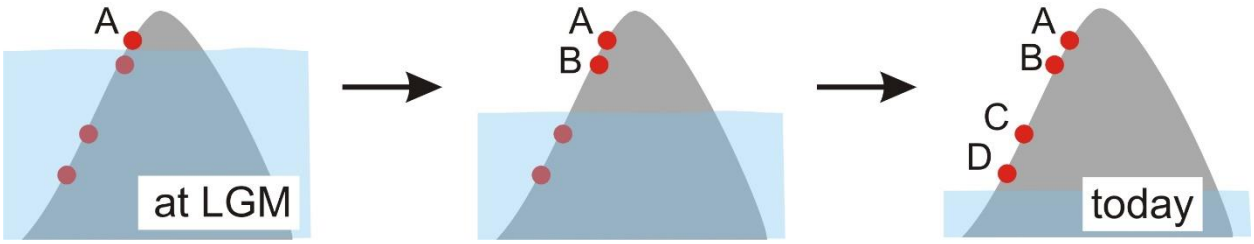

Figure 4: The 'dipstick' method. (a) At the last glacial maximum (LGM), most or all of the sample locations (red dots) were covered by ice to a depth at which the cosmic ray flux was blocked. (b) As the ice surface lowered around the mountain, lower elevations were exposed to cosmic rays. The cosmic rays began reacting with minerals in the now-exposed rock, producing TCNs. (c) Exposure ages calculated for sample sites today will allow for the ice thinning history to be ascertained. Samples A, B, C, and D will have progressively younger exposure ages, respectively. Note: This image was borrowed from an article about Antarctic dipsticks. In New England, mountains were likely overtopped by ice at the LGM and are now completely ice free. Image from: https://www.bas.ac.uk/project/reconstructing-millennial-scale-ice-sheet-change/surface-exposure-dating/

Figure 5: An example of an exposure-age dipstick from Koester et al. (2017). This dipstick was constructed by calculating surface exposure ages for 7 glacially-transported boulders (grey circles) and 9 scoured-bedrock surfaces (black triangles). Error bars indicate internal measurement uncertainty for each exposure age. Gray lines are 1000 age-elevation regressions produced during Monte-Carlo simulations in which each exposure age assumed a random value within its uncertainty, creating a population of possible thinning dates and rates.

Figure 6: Map of dipstick locations for the entire New England dipstick project. Red boxes indicated mountains that will be used to construct dipsticks for this thesis project. Both Cadillac Mountain, ME, and Mt. Washington, NH, have been used to construct dipsticks as part of the New England dipstick project (Koester et al., 2017, ___). Mt. Katahdin, ME was used to construct a dipstick in the 1990s (published in Davis et al., 2015). Note: since the production of this image, Kearsarge Mountain, NH, was replaced by Mt. Monadnock, NH, as a site for dipstick construction.

References:

Abe-Ouchi, A., Saito, F., Kawamura, K., Raymo, M.E., Okuno, J., Takahashi, K., and Blatter, H., 2013, Insolation-driven 100,000-year glacial cycles and hysteresis of ice-sheet volume: Nature, v. 500, no. 7461, p. 190.

Balco, G., 2011, Contributions and unrealized potential contributions of cosmogenic-nuclide exposure dating to glacier chronology, 1990-2010: Quaternary Science Reviews, v. 30, no. 1-2, p. 3-27.

Balco, G., Briner, J., Finkel, R.C., Rayburn, J.A., Ridge, J.C., and Schaefer, J.M., 2009, Regional beryllium-10 production rate calibration for late-glacial northeastern North America: Quaternary Geochronology, v. 4, no. 2, p. 93-107.

Balco, G., Stone, J.O., Lifton, N.A., and Dunai, T.J., 2008, A complete and easily accessible means of calculating surface exposure ages or erosion rates from 10Be and 26Al measurements: Quaternary Geochronology, v. 3, no. 3, p. 174-195.

Balco, G., Stone, J.O.H., Porter, S.C., and Caffee, M.W., 2002, Cosmogenic-nuclide ages for New England coastal moraines, Martha's Vineyard and Cape Cod, Massachusetts, USA: Quaternary Science Reviews, v. 21, no. 20, p. 2127-2135.

Bierman, P.R., Davis, P.T., Corbett, L.B., Lifton, N.A., and Finkel, R.C., 2015, Cold-based Laurentide ice covered New England's highest summits during the last glacial maximum: Geology (Boulder), v. 43, no. 12, p. 1059-1062.

Bierman, P., 2007, Cosmogenic glacial dating, 20 years and counting: Geology, v. 35, no. 6, p. 575-576.

Briner, J.P., Miller, G.H., Davis, P.T., Bierman, P.R., and Caffee, M., 2003, Last Glacial Maximum ice sheet dynamics in Arctic Canada inferred from young erratics perched on ancient tors: Quaternary Science Reviews, v. 22, no. 5, p. 437-444.

Broecker, W.S., 2006, Abrupt climate change revisited: Global and Planetary Change, v. 54, no. 3, p. 211-215.

Buizert, C., Gkinis, V., Severinghaus, J.P., et al., 2014, Greenland temperature response to climate forcing during the last deglaciation: Science, v. 345, no. 6201, p. 1177-1180.

Carlson, A.E., and Clark, P.U., 2012, Ice sheet sources of sea level rise and freshwater discharge during the last deglaciation: Reviews of Geophysics, v. 50, no. 4.

Carlson, A.E., and Winsor, K., 2012, Northern Hemisphere ice-sheet responses to past climate warming: Nature Geoscience, v. 5, no. 9, p. 607.

Carlson, A.E., Clark, P.U., Raisbeck, G.M., and Brook, E.J., 2007, Rapid Holocene deglaciation of the Labrador sector of the Laurentide Ice Sheet: Journal of Climate, v. 20, no. 20, p. 5126-5133.

Clark, P.U. and Tarasov, L., 2014, Closing the sea level budget at the Last Glacial Maximum: Proceedings of the National Academy of Sciences, v. 111, no. 45, p. 15861-15862.

Clark, P.U., Shakun, J.D., Baker, P.A., et al., 2012, Global climate evolution during the last deglaciation: Proceedings of the National Academy of Sciences, v. 109, no. 19, p. E1134.

Clark, P.U., Dyke, A.S., Shakun, J.D., et al., 2009, The Last Glacial Maximum: Science, v. 325, no. 5941, p. 710-714.

Clark, P.U., and Mix, A.C., 2002, Ice sheets and sea level of the Last Glacial Maximum: Quaternary Science Reviews, v. 21, no. 1, p. 1-7.

Clark, P.U., Marshall, S.J., Clarke, G.K.C., Hostetler, S.W., Licciardi, J.M., and Teller, J.T., 2001, Freshwater Forcing of Abrupt Climate Change During the Last Glaciation: Science, v. 293, no. 5528, p. 283-287.

Corbett, L.B., Bierman, P.R., and Rood, D.H., 2016, An approach for optimizing in situ cosmogenic 10Be sample preparation: Quaternary Geochronology, v. 33, p. 24-34.

Davis, P.T., Bierman, P.R., Corbett, L.B., and Finkel, R.C., 2015, Cosmogenic exposure age evidence for rapid Laurentide deglaciation of the Katahdin area, west-central Maine, USA, 16 to 15 ka: Quaternary Science Reviews, v. 116, p. 95-105.

Denton, G.H., Anderson, R.F., Joggweiler, J.R., Edwards, R.L., Schaefer, J.M., and Putnam, A.E., 2010, The Last Glacial Termination: Science, v. 328, no. 5986, p. 1652-1656.

Deschamps, P., Durand, N., Bard, E., et al., 2012, Ice-sheet collapse and sea-level rise at the Bølling warming 14,600 years ago: Nature, v. 483, no. 7391, p. 559-564.

Dyke, A.S., and Gibbard, P.L., 2004, An outline of North American deglaciation with emphasis on central and northern Canada, Elsevier.

Fyke, J.G., Sacks, W.J., and Libscomb, W.H., 2014, A technique for generating consistent ice sheet initial conditions for coupled ice sheet/climate models: Geoscientific Model Development, v. 7, no. 3, p. 1183-1195.

Gosse, J.C., and Phillips, F.M., 2001, Terrestrial in situ cosmogenic nuclides: theory and application: Quaternary Science Reviews, v. 20, no. 14, p. 1475-1560.

Gregoire, L.J., Payne, A.J., and Valdes, P.J., 2012, Deglacial rapid sea level rises caused by ice-sheet saddle collapses: Nature, v. 487, no. 7406, p. 219-222.

Koester, A.J., Shakun, J.D., Bierman, P.R., Davis, P.T., Corbett, L.B., Goehring, B.M., Vickers, A., Zimmerman, S.H., 2017a, Rapid thinning of the Laurentide ice sheet at Mt. Washington, NH, during the Bolling Warming, constrained by analysis of cosmogenic 14C and 10Be: Geological Society of America Abstracts with Programs, v. 49, no. 6.

Koester, A.J., Shakun, J.D., Bierman, P.R., and Davis, P., 2017b, Rapid thinning of the Laurentide Ice Sheet in coastal Maine, USA during late Heinrich Stadial 1: Quaternary Science Reviews, v. 163, p. 180-192.

Lal, D., 1991, Cosmic ray labeling of erosion surfaces: in situ nuclide production rates and erosion models: Earth and Planetary Science Letters, v. 104, no. 2, p. 424-439.

Lambeck, K., Rouby, H., Purcell, A., Sun, Y., and Sambridge, M., 2014, Sea level and global ice volumes from the Last Glacial Maximum to the Holocene: Proceedings of the National Academy of Sciences, v. 111, no. 43, p. 15296-15303.

Liu, Z., Otto-Bliesner, B.L., He, F., et al., 2009, Transient Simulation of Last Deglaciation with a New Mechanism for Bølling-Allerød Warming: Science, v. 325, no. 5938, p. 310-314.

McManus, J.F., Francois, R., Gherardi, J.M., Keigwin, L.D., Brown-Leger, S., 2004, Collapse and rapid resumption of Atlantic meridional circulation linked to deglacial climate changes: Nature, v. 428, p. 834-837.

NGRIP Members, 2004, High-resolution record of Northern Hemisphere climate extending into the last interglacial period: Nature, v. 431, p. 147-151.

Nishiizumi, K., Kohl, C.P., Arnold, J.R., Klein, J., Fink, D., and Middleton, R., 1991, Cosmic ray produced 10Be and 26Al in Antarctic rocks: exposure and erosion history: Earth and Planetary Science Letters, v. 104, no. 2, p. 440-454.

Paterson, W.S.B., 1994. The Physics of Glaciers. Pergamon, Oxford, 480pp

Payne, A.J., 1995, Limit cycles in the basal thermal regime of ice sheets: Journal of Geophysical Research: Solid Earth, v. 100, no. B3, p. 4249-4263.

Peltier, W.R., 2005, On the hemispheric origins of meltwater pulse 1a: Quaternary Science Reviews, v. 24, no. 14, p. 1655-1671.

Phillips, F.M., Leavy, B.D., Jannik, N.O., Elmore, D., and Kubik, P.W., 1986, The Accumulation of Cosmogenic Chlorine-36 in Rocks: a Method for Surface Exposure Dating: Science, v. 231, no. 4733, p. 41-43.

Ridge, J.C., Balco, G., Bayless, R.L., et al., 2012, The new North American Varve Chronology: A precise record of southeastern Laurentide Ice Sheet deglaciation and climate, 18.2-12.5 kyr BP, and correlations with Greenland ice core records: American Journal of Science, v. 312, no. 7, p. 685-722.

Shakun, J.D., Clark, P.U., He, F., et al., 2012, Global warming preceded by increasing carbon dioxide concentrations during the last deglaciation: Nature, v. 484, no. 7392, p. 49-54.

Stokes, C.R., Tarasov, L., Blomdin, R., Cronin, T.M., Fisher, T.G., Gyllencreutz, R., Haatestrand, C., Heyman, J., Hindmarsh, R.C., Hughes, A.L., and Jakobsson, M., 2015, On the reconstruction of palaeo-ice sheets: recent advances and future challenges: Quaternary Science Reviews, v. 125, p. 15-49.